Original Article

Decellularization alters the unfavorable regenerative adverse microenvironment of the injured spinal cord to support neurite outgrowth

Junxia Hu[#], Jianghong Shangguan[#], Parizat Askar, Jinghui Xu, Hualin Sun, Songlin Zhou, Changlai Zhu, Wenfeng Su, Yun Gu^

Jiangsu Key Laboratory of Neuroregeneration, Co-Innovation Center of Neuroregeneration, Jiangsu Clinical Medicine Center of Tissue Engineering and Nerve Injury Repair, Nantong University, Nantong, China

Contributions: (I) Conception and design: Y Gu; (II) Administrative support: None; (III) Provision of study materials or patients: None; (IV) Collection and assembly of data: None; (V) Data analysis and interpretation: J Hu, J Shangguan, P Askar, J Xu; (VI) Manuscript writing: All authors; (VII) Final approval of manuscript: All authors.

[#]These authors contributed equally to this work.

Correspondence to: Wenfeng Su; Yun Gu. Jiangsu Key Laboratory of Neuroregeneration, Co-Innovation Center of Neuroregeneration, Jiangsu Clinical Medicine Center of Tissue Engineering and Nerve Injury Repair, Nantong University, Nantong, China. Email: suwenfeng@ntu.edu.cn; guyun@ntu.edu.cn.

Background: Acellular tissue has been transplanted into the injury site as an external microenvironment to intervene with imbalance microenvironment that occurs after spinal cord injury (SCI) and stimulating axonal regeneration, although the mechanism is unclear. Given decellularization is the key means to obtain acellular tissues, we speculated changes in the internal components of tissue caused by decellularization may be the key reason why acellular tissues affect remodeling of the microenvironment.

Methods: Complete spinal cord crush in a mouse model was established, and the dynamic of extracellular matrix (ECM) expression and distribution during SCI was studied with immunohistochemistry (IHC). Normal spinal cord (NSC) and 14-day injury spinal cord (ISC) were obtained to prepare the decellularized NSC (DNSC) and decellularized ISC (DISC) through a well-designed decellularization method, and the decellularization effects were evaluated by residual DNA content determination, hematoxylin and eosin staining (H&E), and IHC. Rat dorsal root ganglia (DRG) were co-cultured with NSC, ISC, DNSC, and DISC to evaluate their effect on neurite outgrowth. Furthermore, the mechanisms by which decellularized tissue promotes axonal growth were explored with proteomics analysis of the protein components and function of 14-day ISC and DISC.

Results: We found the expression of the four main ECM components (collagen type I and IV, fibronectin, and laminin) gradually increased with the progression of SCI compared to NSC, peaking at 14 days of injury then slightly decreasing at 21 days, and the distribution of the four ECM proteins in the ISC also changed dynamically. H&E staining, residual DNA content determination, and IHC showed decellularization removed cellular components and preserved an intact ECM. The results of co-cultured DRG with NSCs, ISCs, DNSCs, and DISCs showed DNSCs and DISCs had a stronger ability in supporting neurite outgrowth than NSC and ISC. We found through proteomics that decellularization could remove proteins associated with inflammatory responses, scarring, and other pathological factors, while completely retaining the ECM proteins.

Conclusions: Taken together, our findings demonstrate decellularization can optimize the imbalanced microenvironment after SCI by removing components that inhibit spinal cord regeneration, providing a theoretical basis for clinical application of acellular tissue transplantation to repair SCI.

^ ORCID: 0000-0002-3124-6623.

Keywords: Extracellular matrix; decellularization; neurite outgrowth; microenvironment; spinal cord injury

Submitted Jul 22, 2022. Accepted for publication Aug 23, 2022.
doi: 10.21037/atm-22-3969
View this article at: https://dx.doi.org/10.21037/atm-22-3969

Introduction

Traumatic spinal cord injury (SCI) occurs commonly in clinical practice. Due to the extremely limited regenerative capacity of axons in the central nervous system (CNS), the problem of regenerative repair and functional recovery after injury has always been a challenge for regenerative medicine, and there is currently no widely accepted treatment strategy (1). SCI can lead to a complex series of pathophysiological changes, including cell death, axonal degeneration and demyelination, glial scarring, inflammation, and other pathological defects, which in turn lead to an imbalance in the spinal cord microenvironment that is unfavorable for axonal growth (2,3). An unbalanced microenvironment is the main reason for the extremely weak axon regeneration ability and poor functional recovery seen after SCI, and improving the local regenerative microenvironment to support axonal regeneration is very important in its treatment. In recent years, a growing number of studies have been devoted to optimization of the microenvironment by removal of certain inhibitory components such as chondroitin sulfate proteoglycans (CSPGs) and myelin sheath fragments using their antagonist including the CSPG-scavenging agent chondroitinase ABC and myelin-associated glycoprotein antagonists to promote spinal cord regeneration (4-8). On the other hand, researchers have also stimulated axonal regeneration by adding cytokines such as neurotrophic factors (NT3, BDNF, and CNTF) as well as biomaterials such as extracellular matrix (ECM) components (collagen IV, laminin, and periostin) and other nerve regeneration promoters (9-13).

The ECM is the external environment that cells and tissues depend on for survival, activity, and regulation, as well as tissue damage repair and remodeling (14). With this in mind, ECM derived from decellularized tissues including nerves, blood vessels, brain, and spinal cords has been explored as the promoters of spinal cord regeneration (15-19). Xu *et al.* observed that acellular spinal cords could promote vascular remodeling in an SCI model (16), and Cerqueira *et al.* found decellularized peripheral nerve supported implanted cell survival and injured axon regeneration after SCI (17). Further, Bai *et al.* reported decellularized optic nerve facilitated spinal cord axon regeneration and remyelination at the injury site of rat spinal cord (18). Although some achievements have been made in the use of decellularized tissue (i.e., tissue-derived ECM) to repair SCI, more research is required to explore how to better utilize ECM to improve the microenvironment. Therefore, it is of most importance to reveal the mechanism underlying an ECM-optimized microenvironment.

It is well known that an effective decellularization method can not only remove tissue cellular components, soluble proteins, and most immunogens, but also retain tissue-specific structures and physicochemical and biological components including ECM and some functional proteins (20). Crapo *et al.* found the ability of acellular optic nerve, acellular spinal cord, and acellular brain tissue to support PC12 cell proliferation, migration, and differentiation was due to the retention of some neural support proteins such as laminin and some growth factors including vascular endothelial growth factor (VEGF) and basic fibroblast growth factor (bFGF) (21). Sun *et al.* reported decellularization could selectively eliminate some axon growth-inhibiting molecules such as myelin-associated glycoprotein (MAG) and CSPGs and preserve axon-growth-promoting molecules in the ECM such as collagen type IV and laminin (22). Based on these studies, we speculated decellularization may be the reason why tissue-derived ECM can effectively promote nerve growth or regeneration because it can remove some of the nerve growth inhibitory components in tissue while retaining effective components that are beneficial to spinal cord regeneration.

In this study, we used a mouse SCI model to observe dynamic changes of the ECM during injury and prepared decellularized normal spinal cord (DNSC) and decellularized injured spinal cord (DISC) from mice through a combined decellularization method using normal spinal cord NSC and 14-day injury spinal cord (ISC). Rat dorsal root ganglia (DRG) were co-cultured with NSC, ISC, DNSC, and DISC to evaluate their effect on neurite outgrowth, and we found DNSC and DISC had stronger

ability in supporting neurite outgrowth than NSC and ISC. We also performed proteomics to compare the protein components of ISC and DISC and found decellularization could remove axon growth inhibitory proteins such as dysregulated CSPGs. The data collectively demonstrate decellularization can optimize the microenvironment that inhibits spinal cord regeneration, providing a theoretical basis for the clinical application of acellular tissue transplantation to repair SCI. We present the following article in accordance with the ARRIVE reporting checklist (available at https://atm.amegroups.com/article/view/10.21037/atm-22-3969/rc).

Methods

Animals and SCI model preparation

Healthy adult male Institute of Cancer Research (ICR) mice (7-week-old, 20–25 g) were provided by the Experimental Animal Center of Nantong University and housed in temperature- and humidity-controlled conditions with a 12-hour light/dark cycle. All animal experimental procedures and protocols were performed under a project license (No. S20210302-037) granted by the Nantong University Animal Experimental Ethics Committee, in compliance with the Institutional Animal Care and Use Committee (IACUC) of Nantong University. A protocol was prepared before the study without registration.

Mice (n=72) were randomly divided into an SCI group (n=52) and a sham group (n=20). In the SCI group, and on the 1st, 3rd, 7th, and 21st days of injury, 20 mice were placed into four groups, with five mice in each group used for immunohistochemistry (IHC); 32 mice on the 14th day after injury, 5 mice for IHC, 15 mice for decellularization experiments, and 12 mice for proteomics analysis of the protein components and function of 14-day injury spinal cord before and after decellularization (i.e., ISC and DISC). In the sham-operated group, five mice were subjected to IHC, and 15 were used for decellularization experiments. Prior to surgery and during surgery, mice were under deep anesthesia with 3% isofluorane and placed on a heating pad to maintain their body temperature. Complete spinal cord crush was performed following a previously described method (23). In brief, a midline incision of approximately 1.5 cm was made over the thoracic spine under a dissection microscope, and fat and muscle were removed from thoracic vertebrae 9 and 10 (T9, T10). A laminectomy was performed using a rodent stereotaxic apparatus at the T10 thoracic level to expose the spinal cord and a crush injury was made with a No. 5 Dumont forceps with a tip width of 2 mm. Compression of the intact spinal cord from both sides for 5 s was performed to produce a uniform 2 mm lesion to ensure complete pinching of the cord, and the tip of the forceps were gently scraped through the bone on the ventral side of the vertebral canal to avoid residual spinal cord tissue on the ventral side. Postoperatively, the muscle layer and skin were sutured with 6.0 absorbable sutures. During recovery and testing, mice were housed at an ambient temperature of 24 ℃ and 60% humidity on a 12 h light/dark cycle with ad libitum access to food and water and administered with painkillers and antibiotics. To ensure mice urinated, manual bladder compressions three times a day was performed after surgery.

Preparation of decellularized mice spinal cords

Fresh spinal cords, both normal and injured, were collected from euthanized adult ICR mice (7-week-old, male, n=30) with a protocol approved by the IACUC of Nantong University. Before decellularization, the cords were cleaned with a pre-chilled HBSS to remove blood, then stored at −80 ℃. A combination of physical, chemical, and enzymatic decellularization methods were used to decellularize spinal cord tissues according to a previous description with some modification (24,25). Briefly, each spinal cord was bathed overnight at 4 ℃ in ddH_2O containing 2% penicillin-streptomycin (#15140122, Gibco, Waltham, MA, USA) and gentamicin (100 μg/mL; #15750060, Gibco)/amphotericin solution (2.5 μg/mL; #15290018, Gibco) in a 5 mL tube. The tubes were then placed on a shaker (Allsheng OS-100, Hangzhou, China) and shaken at 60 rpm/min for 2 hours at room temperature. To remove cellular substances, the tissues were sequentially washed three times with 3% (v/v) Triton X-100 (#9036-19-5, Sigma-Aldrich, St. Louis, MO, USA) containing 1% penicillin-streptomycin (Gibco) for 2 h and 2% sodium deoxycholate solution (#A0405759, Acros Organics, Geel, Belgium) for 4 hours at room temperature (the liquid was exchanged every 1 h). Following three washes with ddH_2O for 10 min each time to remove residual substances, the tissues were treated with the enzyme treatment mixture consisting of 50 units/mL DNase (#11284932001, Sigma-Aldrich) and 10 μg/mL RNase (#11119915001, Sigma-Aldrich) for 2 h at 37 ℃. DNSC and DISC were then bathed in 100% alcohol at room temperature at 50 rpm/min for 12 h followed by washing three times for 10 min each time, then lyophilized

for storing at –20 ℃ until use.

Characterization of decellularized spinal cord

Hematoxylin and eosin (H&E) staining, IHC, and residual DNA content determination were performed to verify decellularization effects. For H&E staining, NSC) and decellularized spinal cord (DSC) were fixed in 4% paraformaldehyde for 4 h, and after three washes with phosphate buffer solution (PBS), were paraffin-embedded, sectioned, and stained with H&E (#C0105M, Beyotime, Shanghai, China). For the IHC, NSCs and DSCs were embedded in the optimal cutting temperature compound (OCT; #4583, Sakura, Tokyo, Japan) and cut longitudinally into 20-μm-thick slices using a freezing microtome (Thermo Fisher, Waltham, MA, USA). Details of the IHC procedure are described below in Section 2.6. To determine residual DNA content in DSC, NSC and DSCs were digested in 0.3 mg/mL papain solution (#9001-73-4, Sigma), and residual DNA was then quantitatively assessed by a Quant-iT picoGreen kit (#P11495, Invitrogen, Waltham, MA, USA) following the manufacturer's procedure. DNA extracts were subjected to gel electrophoresis on 1.0% agarose gel followed by imaging with ultraviolet transillumination.

Preparation of tissue sections and sterilization

NSC, ISC, DSC, and DISC were embedded in frozen PBS, then cut longitudinally into 50-μm-thick slices using a freezing microtome (Thermo Fisher). Slices were attached to the bottom of a 24-well plate (Corning, NY, USA) and stored in a –20 ℃ freezer. Before use, the plate was sterilized by ultraviolet light in a biosafety cabinet (ESCO, Singapore) for 30 min, then washed three times for 10 minutes each with DMEM containing 1% penicillin-streptomycin.

DRG isolation and ex vivo culture on DSCs and NSCs

Embryonic day (E) 15 SD rats were used for DRG extraction as previously described (24). In brief, pregnant SD rats were euthanized by CO_2 and embryos were removed. After the removal of redundant roots in a precooled Hank's Balanced Salt Solution (HBSS; #14185052, Invitrogen) under a stereoscopic microscope, DRG explant was seeded onto 24-well plates which were pre-coated with slices of the DSCs (n=5) and NSCs (n=5). Plates were then incubated at 37 ℃ for 12 hours with an adherent medium consisting of DMEM medium (#11965092, Gibco), 5% FBS (#10099141C, Gibco) and 1% penicillin-streptomycin. After removing the supernatant, DRG blocks were continually cultured with the growth medium containing neurobasal medium (#10888022, Gibco), 2% B27 supplement (#17504044, Gibco), 50 ng/mL NGF (#N2513, Sigma), 2 mM L-glutamine (#25030081, Gibco), and 1% penicillin-streptomycin at 37 ℃ with 5% CO_2 and 92% humidity.

Immunocytochemistry and immunohistochemistry

Spinal cords were post-fixed in 4% paraformaldehyde (PFA; #P0099, Byotime) and embedded into OCT (Sakura), then cut into 30 μm-thick slices with a cryostat and processed for IHC. For immunocytochemistry (ICC), cells were fixed with 4% PFA in PBS for 30 minutes at room temperature, ready for ICC. Slides and cells were rinsed three times with PBS for 10 min each time, then permeabilized and blocked with 10% donkey serum (#D9663, Sigma) in PBS containing 0.3% Triton X-100-T for 1 hour at room temperature before incubation with primary antibodies overnight at 4 ℃. The following primary antibodies were used: β-III tubulin (TuJ1, 1:250; #MMS-435P, Covance, Princeton, NJ, USA), laminin (1:300; #ab11575, Abcam, Cambridge, MA, USA), collagen I (1:300; #orb500936, Biorbyt, Cambridge, UK), AF488 conjugate collagen IV (1:300; #1340-30, SouthernBiotech, Birmingham, AL, USA), fibronectin (1:100; #LS-C85816, LSBio, Seattle, WA, USA). The following secondary antibodies were applied for 1 h at room temperature: Alexa Fluor® 488 AffiniPure donkey anti-mouse (#715-545-151, Jackson Immunoresearch, West Grove, PA, USA), Alexa Fluor® 488 AffiniPure donkey anti-rabbit (#711-545-152, Jackson), Cy™3 AffiniPure donkey anti-mouse (#715-165-151, Jackson), Cy™3 AffiniPure donkey anti-rabbit (#711-165-152, Jackson), and diluted 1:1,000. For each staining, samples from at least three individual animals per group were processed simultaneously and used for the analysis. Sections and cells were rinsed three times with PBS for 10 min before Hoechst33342 (#875756-97-1, Sigma) staining and mounting. Immunofluorescence of the stained sections was imaged under a Zeiss Observer fluorescence microscope (Carl Zeiss Microscopy, Heidenheim, Germany).

Proteomic analysis

Proteomic analysis was performed to assess the protein components from ISCs (n=3) and DISCs (n=3) and was

provided by Oebiotech, a company we commissioned (https://www.oebiotech.com). Briefly, the trypsin-digested peptides were labeled with TMT-10-plex isobaric labeling kits (# A37725, ThermoFisher) according to the manufacturer's instructions then analyzed on an AB SCIEX nanoLC-MS/MS system (Triple TOF 6600, AB SCIEX, USA). Protein identification was analyzed using ProteinPilot software (v5.0, AB SCIEX, USA) integrating the paragon algorithm against the Unified Protein Database (UniProt; https://www.uniprot.org/), and protein quantification was analyzed with Skyline software (v3.6, AB SCIEX, USA). After searching the decoy concatenated uniprot rat protein database using the integrated PSPEP tool in ProteinPilot software, the local false discovery rate (FDR) was estimated to be 1.0%, and the proteins with global FDR ≤1% and unique peptides ≥1 were considered for further analysis of differentially expressed proteins (DEPs). Fold changes (FCs) were calculated by comparing the averaged IDSC group to the averaged DSC group, and P values were obtained by using the Student's *t*-test, and the proteins with FC >1.5 and P<0.05 were considered DEP compared to the control.

Statistical analysis

Data are reported as the mean ± standard error and analyzed using GraphPad Prism version 8.0.1 (GraphPad Software, CA, USA). Student's t-test (two-tailed) was using to compare continuous variables between two groups. Corrected P values <0.05 were considered statistical significance.

Results

Dynamic changes of the ECM expression and distribution during the SCI

The ECM of a tissue provides structure and organization to maintain tissue stability and helps regulate resident cell function and intercellular communication. After SCI, ECM breakdown leads to the destruction of neural tissues, and the instability or alteration of its structure and chemical composition affects the migration, communication, and survival of neural and non-neural cells critical for spinal cord repair, undoubtedly leading to regeneration failure (26). Based on this, we first observed the dynamic changes of ECM expression and distribution during SCI. As collagens, fibronectin, and laminin are the main ECM components in NSC, we examined their expression and distribution by IHC in the NSC and injured 1, 3, 7, 14, and 21 days spinal cord. As shown in *Figures 1*,*2*, the expression of collagen type I and IV, fibronectin, and laminin gradually increased with the progression of SCI and repair compared to uninjured spinal cord, peaking at 14 days of injury then slightly decreasing at 21 days of injury. Of particular note is the dynamically changing distribution of these four ECM proteins during SCI. Specifically, in normal spinal cord, they are evenly distributed to maintain its structure and function. On the first day after SCI, they aggregated on the upper and lower sides of the injury site and started to gradually migrate from both sides of the wound to the injury site on the third day of injury. They continued to migrate to the injury site on days 7–14 of injury and became increasingly dense until fully clustered at the site on day 21 of injury. This dynamic change is consistent with the formation and maturation of glial scars after SCI, which sees pre-scar tissue begin to form at the injury site at 7 days and scar maturation at 14–21 days post SCI. Taken together, we deemed the remodeling of the ECM after SCI affects cell migration, distribution, and formation of glial scars that affect SCI repair.

Characteristics of decellularization efficacy

DSCs were obtained using a combination of physical, chemical, and enzymatic decellularization methods (*Figure 3A*). Given the success of decellularization depends on the following four key criteria: (I) no visible nuclei remain in the tissue after staining with H&E; (II) dsDNA content <50 ng/mg (lyophilized weight); (III) no DNA fragments <200 bp can be observed on agarose gel electrophoresis; (IV) no damage to matrix proteins in decellularized tissue, we evaluated the decellularization efficacy by using H&E staining, IHC, and residual DNA content determination (*Figure 3*). Quantification of dsDNA showed DSCs retained <20 ng dsDNA per mg freeze-dried DSC (*Figure 3B*), suggesting almost all cellular DNA was removed with little remaining in the DSC. H&E staining showed no residual nuclei were visible in the DSC (*Figure 3C*), indicating the cellular components of spinal cord tissue had been removed after decellularization. Immunostaining of DSCs with antibodies against collagen type IV and laminin showed after decellularization treatment, the major ECM proteins of the spinal cord remained intact (*Figure 3D*), suggesting the spinal cord-

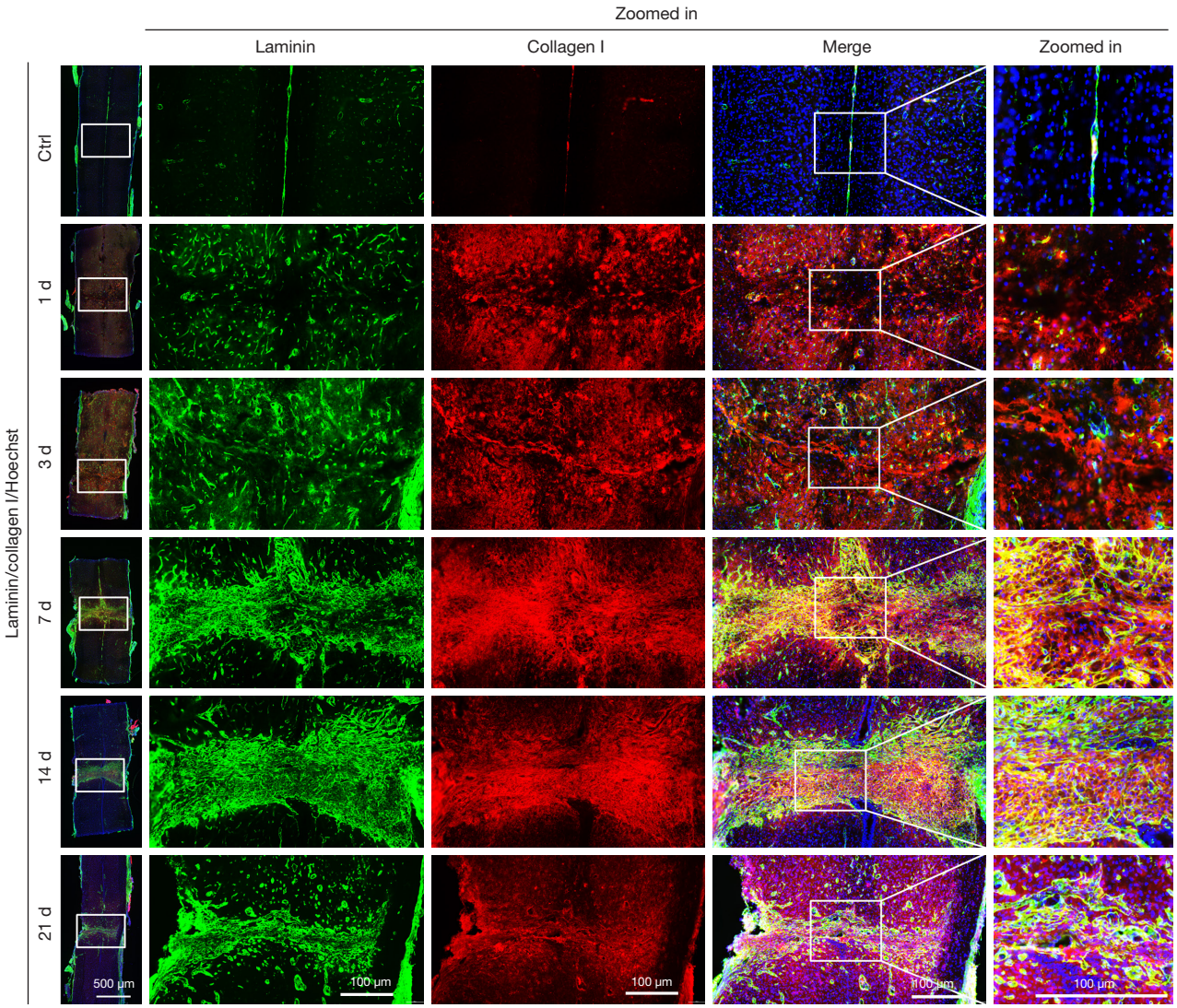

Figure 1 Expression dynamics of collagen I and laminin in a mouse SCI model. Immunofluorescence staining of collagen I (red) and laminin (green) in injured spinal cord sections (1, 3, 7, 14, and 21 days after injury) and normal spinal cord (Ctrl) of mice; scale bars 500 μm. Zoomed in shows high magnification image of the part in the white box; scale bars 100 μm. SCI, spinal cord injury; Ctrl, control.

derived ECM was not disrupted by decellularized agents, and its biological activity and spatial conformation were maintained. In conclusion, we considered the decellularization method used in this study effectively removes cellular components from the spinal cord without disrupting the ECM proteins of DSC.

Decellularization of the NSC and ISC favors DRG neurite outgrowth

To assess the effect of NSC and ISC on neurite outgrowth before and after decellularization, we cultured DRG tissue on longitudinal tissue sections of NSC, ISC, DNSC, and DISC. After 72 hours of culture, cells and tissues were fixed, and neurites were immunofluorescently labeled with β-tubulin III (also known as Tuj1, a neuronal marker), while the four culture substrates were labeled with laminin. Neurite outgrowth was then observed under a fluorescence microscope (*Figures 4*,*5*). As shown in *Figure 4*, although DRG cultured on both NSC and DNSC had neurite outgrowth, the neurites of DRG cultured on NSC could only grow along the connective tissue septum between

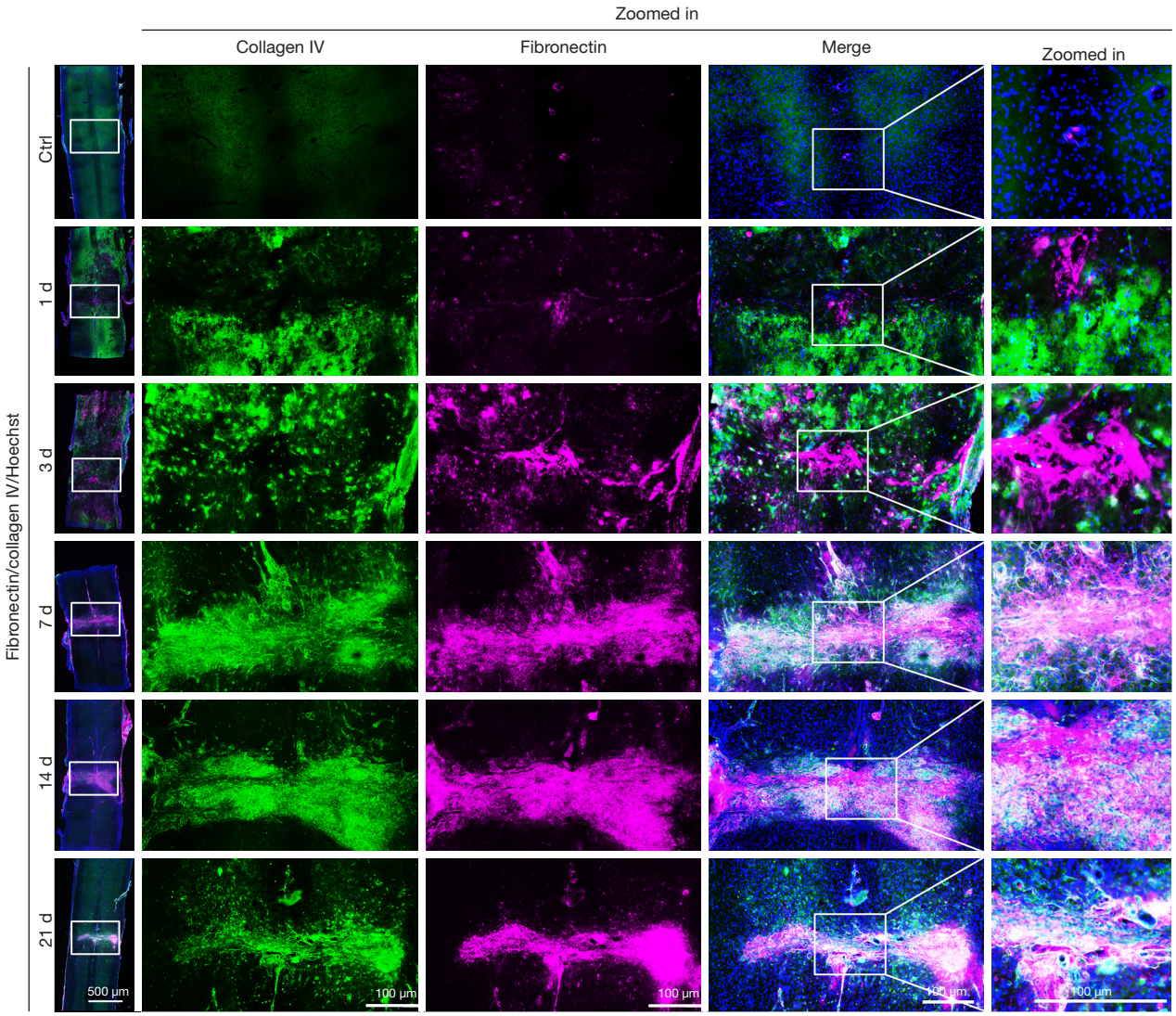

Figure 2 Expression dynamics of collagen IV and fibronectin in a mouse SCI model. Immunofluorescence staining of collagen IV (red) and fibronectin (purple) in ISC sections (1, 3, 7, 14, and 21 days after injury) and NSC (Ctrl) of mice; scale bars, 500 μm. Zoomed in shows high magnification image of the part in the white box; scale bars 100 μm. SCI, spinal cord injury; NSC, normal spinal cord; Ctrl, control.

the two, rather than extending outward (white arrows in *Figure 4*), which may be due to the presence of inhibitory components in non-decellularized NSC blocking neurite extension toward them. In contrast, neurites of DRG cultured on DNSC grew profusely and could extend on DNSC, possibly because decellularization removed components inhibiting neurite outgrowth and extension. Interestingly, DRG cultured on ISC had no neurite outgrowth at all, while that cultured on DISCs not only had abundant neurite outgrowths, but could grow across the glial scar, indicating decellularization could remove the components inhibiting neurite outgrowth in ISC tissue (including the glial scar) and promote nerve growth (*Figure 5*). Therefore, we believed that different neurite outgrowth behavior of DRG cultured on spinal cord tissue before and after decellularization (NSC and DNSC, or ISC and DISC) may be due to changes in protein composition caused by the decellularization process.

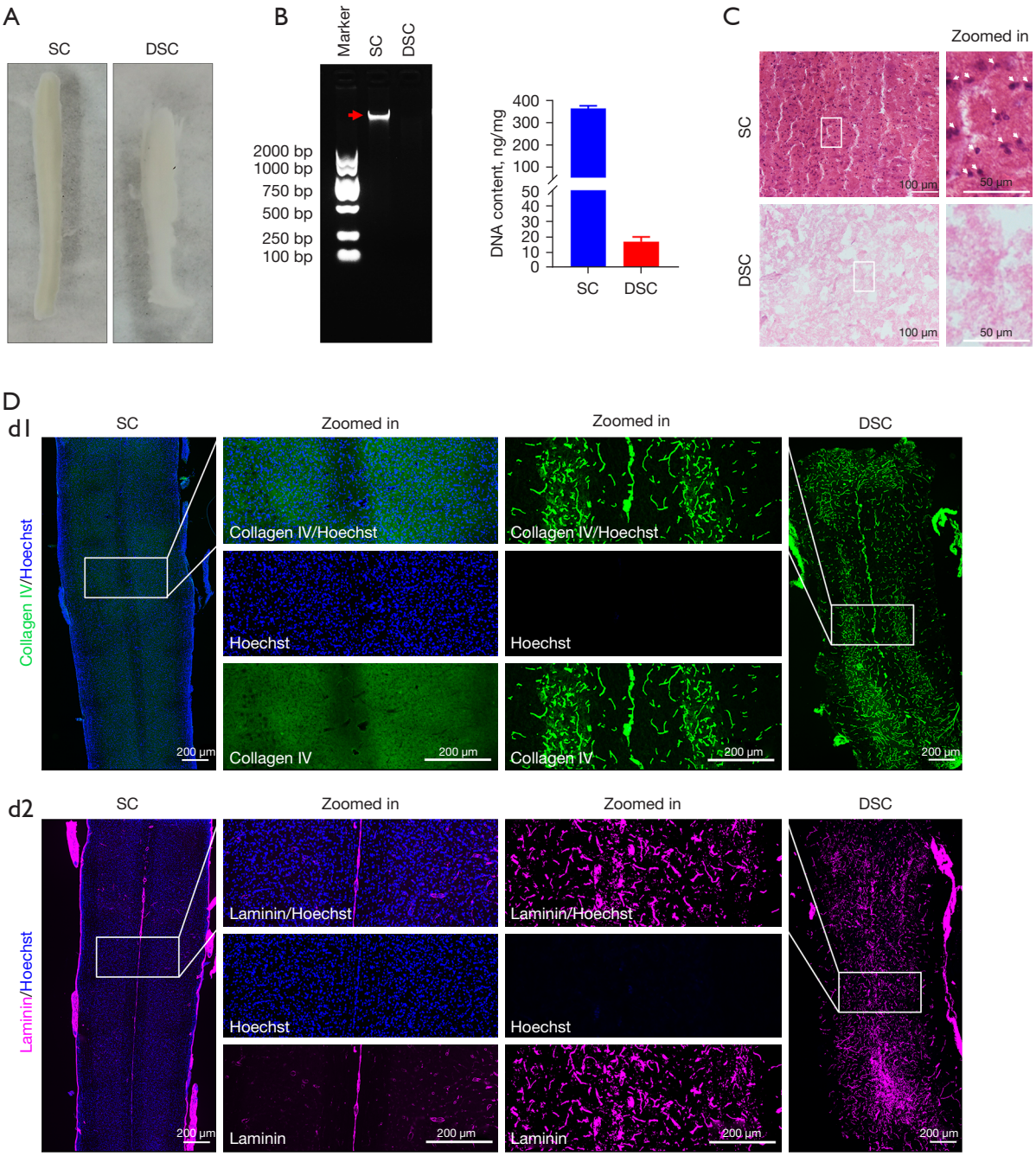

Figure 3 Characterization of the decellularized spinal cords. (A) Morphological observation of the SC and DSC. (B) DNA content detection. The DNA agarose gel electrophoresis map (left) and DNA quantification (histogram, right) shows SC contained high concentrations of DNA (denoted with red arrow) while almost no DNA was detectable in DSC, implying decellularization had removed DNA from the SC. n=5. (C) H&E staining shows morphological observation of the SC and DSC, and shows cell nuclei (denoted with white arrows) are visible in SC but not in DSC, suggesting decellularization had completely removed cellular components from the SC; scale bars, 100 μm. Zoomed in shows the magnified image in the white boxes; scale bars, 50 μm. (D) Immunohistochemical detection of collagen IV (d1, green) and laminin (d2, purple) expression in SC tissue before and after decellularization. Hoechst (blue) marks the cell nuclei. Zoomed in shows high magnification image of the part in the white box; scale bar, 200 μm. SC, spinal cord; DSC, decellularized spinal cord.

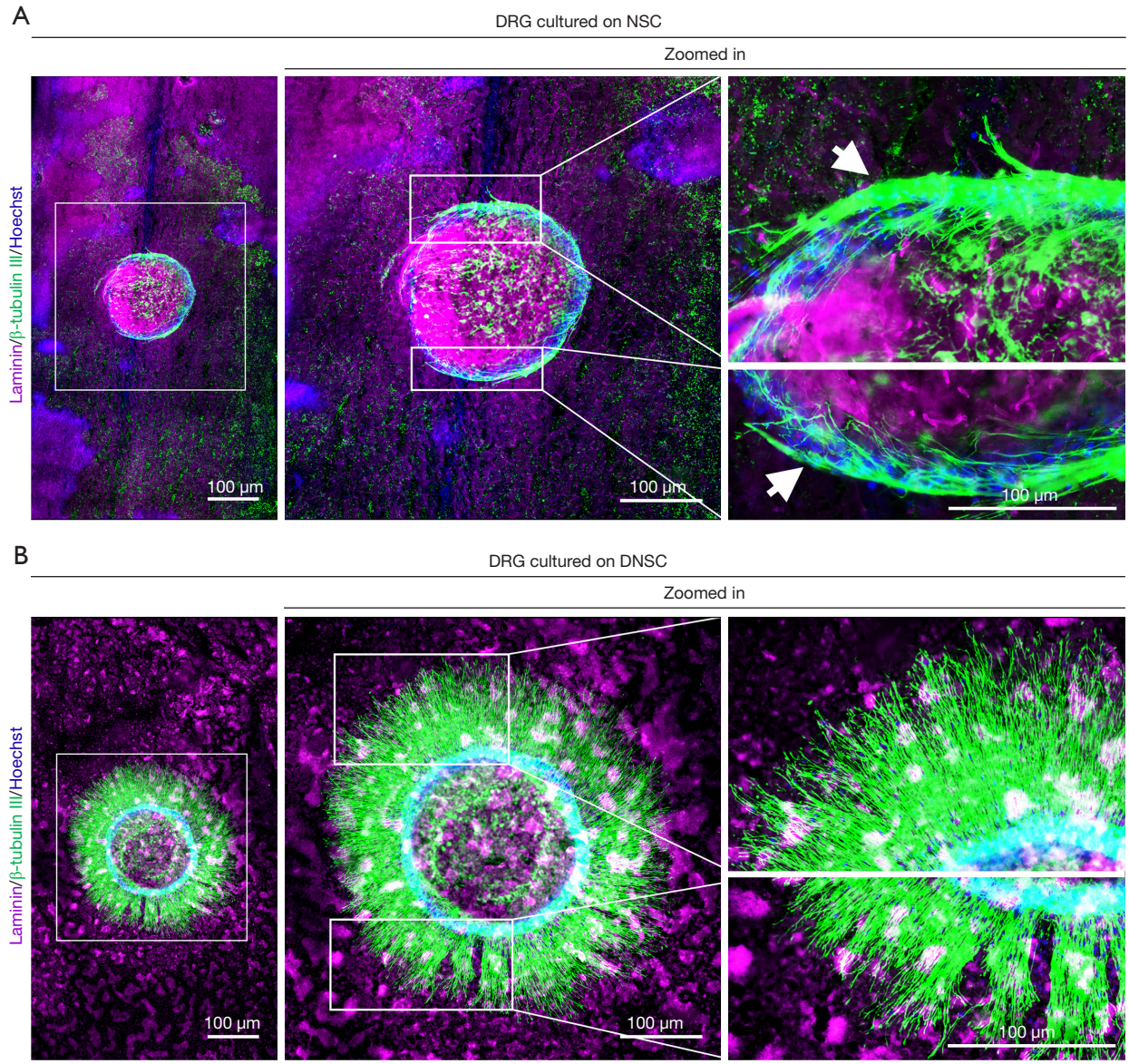

Figure 4 Effects of NSC and DNSC on DRG neurite outgrowth. (A) Immunofluorescence staining for β-tubulin III (a neuronal marker, green) and laminin (purple, indicating NSC) shows outgrowth of DRG neurites cultured on NSC. Neurites are seen growing out of the DRG tissue, but they cannot extend outwards, probably because some repulsive factor in the NSC prevents them from extending; scale bars 100 μm. Zoomed in shows high magnification image of the part in the white box; scale bars 100 μm. White arrows indicate neurites growing from the DRG. (B) Immunofluorescence staining of β-tubulin III (green) and laminin (purple, indicating DNSC) shows DRG neurite outgrowth on DNSC. Numerous neurites can be seen growing out of the DRG tissue and extending outward on the DNSC, presumably because decellularization removes factors that prevent them from extending; scale bars, 100 μm. Zoomed in shows high magnification image of the part in the white box; scale bars 100 μm. NSC, normal spinal cord; DNSC, decellularized normal spinal cord; DRG, dorsal root ganglion.

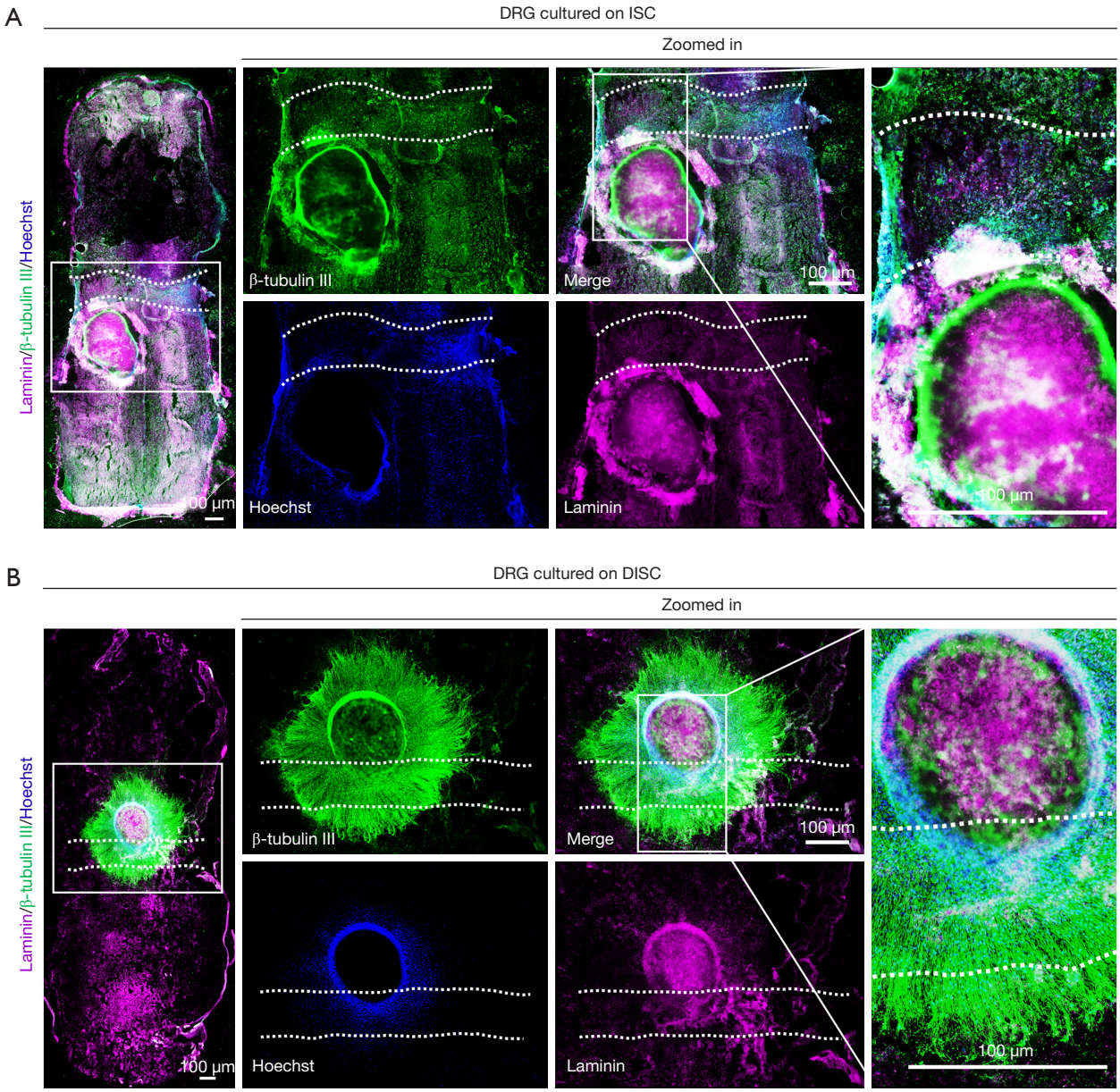

Figure 5 Effects of ISC and DISC on DRG neurite outgrowth. (A) Immunofluorescence staining for β-tubulin III (green, marking neurons) and laminin (purple, indicating NISC) shows no neurites grew out from DRG cultured on ISC. Hoechst labels nuclei. White dotted lines mark the SCII site; scale bars 100 μm. Zoomed in shows a high magnification image of the part in the white box; scale bars 100 μm. (B) Immunofluorescence staining for β-tubulin III (green) and laminin (purple, indicating DISC) shows numerous neurites outgrowth from DRG cultured on DNSC which can extend outward on the DISC across the glial scar. Hoechst labels nuclei. White dotted lines mark the SCI site; scale bars 100 μm. Zoomed in shows high magnification image of the part in the white box; scale bars 100 μm. ISC, injured spinal cord; DISC, decellularized injured spinal cord; DRG, dorsal root ganglion.

Decellularization of ISC selectively removes some axon growth-inhibiting molecules

We next performed proteomic analysis of 14-day injury spinal cord tissue before and after decellularization (i.e., ISC and DISC, three replicates per group) using the multiplexed TMT 10-plex, comparing the differences in protein composition between ISC and DISC to decipher the molecular mechanisms by which decellularization tissue promotes neurite outgrowth. As shown in the Venn diagram of *Figure 6A*, a total of 3,658 proteins were identified in ISC with a false discovery rate (FDR) <1% (https://cdn.amegroups.cn/static/public/atm-22-3969-1.xlsx), and 743 proteins were identified in DISC (https://cdn.amegroups.cn/static/public/atm-22-3969-2.xlsx), indicating there were 2,915 proteins removed in ISC through the decellularization. GO functional analysis of these 2,915 proteins found the top ten GO functions associated with inflammatory response, positive regulation of macrophage chemotaxis, positive regulation of apoptotic cell clearance, astrocyte cell migration, and oxidation-reduction process, suggesting decellularization can remove some factors that are unfavorable for repair in the ISC, such as inflammation, axonal degeneration, scar formation, and other pathological factors (*Figure 6Bb1* and https://cdn.amegroups.cn/static/public/atm-22-3969-3.xlsx). In addition, GO analysis was performed on the 743 proteins in DISC and showed the top ten GO terms of these proteins were mainly enriched in ECM, basement membrane, and proteinaceous ECM, indicating acellular tissue DISC mainly contains matrix proteins while most cellular components had been removed by decellularization (*Figure 6Bb2* and https://cdn.amegroups.cn/static/public/atm-22-3969-4.xlsx). Furthermore, we screened the ECM proteins in ISC and DISC using the MatriSomeDB filtering, and found they shared 100% of the matricellular proteins, with both containing 116 identical matrix proteins including core matrisome (e.g., collagens, laminins, and fibronectins), matrisome-associated proteins (e.g., ECM regulators including Serpin family and Adam family), and secreted factors such as S100 family as well as Cntf and Hbegf (*Figure 6C* and https://cdn.amegroups.cn/static/public/atm-22-3969-5.xlsx). This further illustrated our decellularization method not only removed the components of the ISCs that were not conducive to regeneration, but also completely preserved the ECM proteins. Considering the content of ECM proteins (such as collagen, laminin, fibronectin, and CSPG family) can directly affect the biological behavior of resident cells (such as glial cell proliferation, migration, and scar formation), we further analyzed and compared the differences of ECM protein contents in the SCs before and after decellularization. As shown in *Figure 6D* and https://cdn.amegroups.cn/static/public/atm-22-3969-6.xlsx, the ECM proteins facilitating axon growth and extension, such as collagens, laminins, fibronectin 1 (Fn1), and tenascin C (TNC) were at higher levels in DISC than in ISC. In contrast, proteins that inhibit axonal growth and extension including CSPG family [e.g., versican (Vcan), aggrecan core protein (Acan), biglycan (Bgn), clusterin (Clu), tenascin R (Tnr), and decorin (Dcn)], myelin-associated glycoprotein (MAG), osteoglycin (Ogn), as well as periostin (Postn)] were presented at lower levels in DISC than in ISC. Additionally, the results of CSPG immunostaining showed CSPG was highly expressed in the injury site and its upper and lower sides in ISC, forming relatively dense glial scars, while in DISC, the expression of CSPG was drastically reduced and the dense scars were disintegrated by decellularization (*Figure 6E*). Collectively, those data further confirmed decellularization could remove or decrease the contents of ISC blocking axonal growth or regeneration.

Discussion

Tissues and organs are complex three-dimensional structures composed of a variety of cells and the coordinated action of their surrounding ECM. ECM is the external environment that resident cells and tissues depend on for survival, activity, damage repair, and remodeling (27,28). In the CNS, ECM dysregulation has been recognized as a major factor leading to irreversible changes in the tissue-remodeling microenvironment following injury, directly impairing the inherent ability of neural tissue to regenerate and repair (29,30). In recent years, acellular tissue (tissue-derived ECM) have been transplanted into the injury site as an external microenvironment to intervene in the remodeling process that occurs after injury, stimulating axonal regeneration (31,32). However, the mechanism is unclear. Given acellular tissues were obtained by decellularization, we speculated the changes in the internal components of tissue after decellularization may be the key reason why it affects the remodeling of the microenvironment. Here, we demonstrated decellularization of injured or normal spinal cord tissues can selectively preserve the ECM proteins that facilitate cell growth, while removing axon arresting proteins (e.g., CSPGs, Postn and

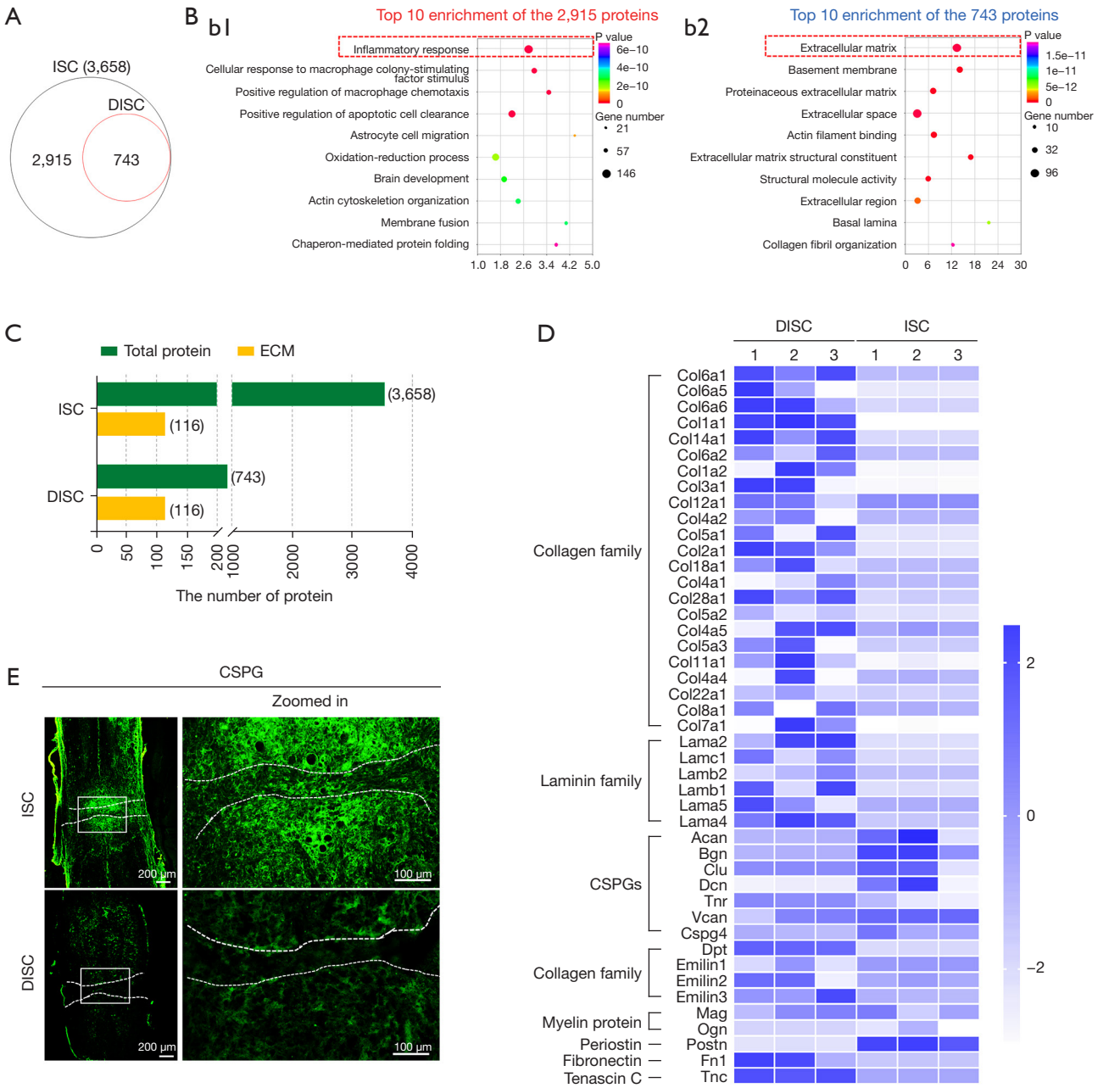

Figure 6 Proteomic analysis of ISC and DISC and IHC validation analysis results. (A) Venn diagram showing the number of proteins detected by mass spectrometry in the ISC and DISC groups. DISC, 743; ISC, 3,658. (B) (b1) GO analysis of the function of 2,915 proteins removed by decellularization in the ISC. The top 10 GO terms are shown in the figure, and the red dotted box marks the first GO function, that is, inflammatory response. (b2) GO analysis of the functions of 741 proteins in the DISC. The top 10 GO terms are shown in the figure, and the red dotted box marks the first GO function, that is, ECM. (C) Histogram showing the number of total and ECM proteins detected in the ISC and DISC groups. (D) Heatmap showing the ratio of protein expression in DISC relative to ISC. (E) Immunofluorescence staining of CSPG (green) in ISC and DISC sections. White dotted lines mark the SCI site; scale bars 200 μm. Zoomed in shows a high magnification image; scale bars 100 μm. ISC, injured spinal cord; DISC, decellularized injured spinal cord; IHC, immunohistochemistry; GO, gene ontology; ECM, extracellular matrix; CSPG, chondroitin sulfate proteoglycan.

MAG) to optimize the adverse microenvironment that inhibits neuronal tissue growth. This finding is consistent with a previous study showing optic nerve decellularization alters the axon-inhibited microenvironment to support neurite outgrowth (22).

Numerous researchers have found the ECM of the CNS is a highly regulated system containing collagens, non-collagens, glycoproteins, hyaluronic acids, proteoglycans, and other factors which play a crucial role in neuronal plasticity and neurite outgrowth. Dysregulation of the ECM composition, abundance, distribution, and stiffness will result in abnormal or absent function of tissues (27), such as neurodegenerative diseases including Alzheimer's disease structure (33). Conversely, tissue lesions or damage can also lead to ECM abnormalities. In NSC, ECM molecules such as CSPG, tenascins, and semaphorins form stable networks around neuronal cell bodies and proximal dendrites, maintaining their structure and function (29). After SCI, ECM dynamic dysregulation (e.g., up-regulation of CSPGs and semaphorins, which inhibit regeneration of damaged axons, and down-regulation of tenascins, which favor axonal regeneration), affects spinal cord regeneration and functional recovery (30,32). In this study, we used a mouse SCI model and IHC to observe dynamic changes in the expression and distribution of major ECM proteins such as collagen type I and IV, laminin, and fibronectin during injury, and found these four ECM molecules were highly expressed and remodeled in and around the injury site (*Figures 1*,*2*). Specifically, early on (1–3 days of injury), the four proteins were expressed and distributed on the upper and lower sides of the injury site (i.e. lesion border), while in the middle and late stages of injury (7–21 days after injury), they were highly expressed and tightly aggregated to the injury site (i.e. lesion core). This suggests the mature glial scars contain not only a high concentration of CSPGs, but a large amount of major ECM proteins such as collagen types I and IV, laminin and fibronectin, providing a dense and stiff mechanical barrier to prevent axon regeneration, although appropriate concentration of the four ECM proteins has been shown to promote neurite outgrowth (34). Removal or reduction of excess ECM proteins in glial scars is one factor promoting spinal cord regeneration (35,36). Numerous studies have shown that depletion or reduction of CSPG expression with chondroitinase ABC (ChABC, a CSPG scavenger) at the site of SCI significantly increases axonal sprouting, growth, and plasticity (7,37). Here we used a well design decellularization method (the decellularization effects have been evaluated by H&E, IHC, and DNA content detection, *Figure 3*) to selectively remove the dysregulated ECM proteins or other molecules that inhibit neuronal regeneration from NSC and ISC and resulting DNSC and DISC, and co-cultured them with DRG explants to evaluate their effect on neurite outgrowth. We found the DNSC and DISCs had stronger ability in supporting neurite outgrowth than NSC and ISC, suggesting decellularization can indeed remove the axon growth inhibitory proteins (*Figures 4*,*5*). To further confirm this, we used proteomics to compare the protein components of 14-day ISC and DISC, and found the top ten GO functions of the 2,915 proteins removed from ISC by decellularization were enriched in the inflammatory response, the infiltration of macrophages, and the activation of astrocytes, while the top ten GO terms of 743 proteins retained in DISC included ECM and basement membrane (*Figure 4A-4C*). As inflammatory response is an important cause of the imbalance of the spinal cord microenvironment after SCI (3,38), we deemed decellularization can remove the factors that are unfavorable for spinal cord repair and optimize the inhibitor microenvironment to become a balance microenvironment or even a promoting microenvironment. Using MatriSomeDB filtering, we found the types of ECM proteins between the ISC and DISC were exactly the same, but the content was different, in that both contained 116 identical matrix proteins (*Figure 6C* and https://cdn.amegroups.cn/static/public/atm-22-3969-5.xlsx), further illustrating decellularization not only removed the inhibitory components of the ISC that are not conducive to regeneration, but also preserved the ECM proteins intact despite their differences in content. Next, we comparatively analyzed the differences in ECM protein contents between ISC and DISC and found DISC had a high abundance of ECM proteins that facilitate axon growth and extension, such as collagens, laminins, Fn1 (39), and TNC (40), and low level ECM proteins that inhibit axonal growth and extension including CSPG4 (6,41), Vcan (42), Acan (43), Bgn (44), Clu (45), Tnr (46), Dcn (47), MAG, and Postn (48). However, in ISC, the expression of these proteins was the opposite of that in DISC, with high expression of axonal growth inhibitory molecules and low expression of promoting molecules (*Figure 6D* and https://cdn.amegroups.cn/static/public/atm-22-3969-6.xlsx), further demonstrating decellularization could remove or decrease the contents arresting axonal growth or regeneration. Moreover, we found the expression of CSPG in DISC was drastically reduced, and its dense organization was disintegrated by decellularization

(*Figure 6E*), suggesting decellularization can also alter the stiffness and density of the glial scar, making it soft and favorable for axons to pass through the scar. This supports our previous results that neurites of DRG plants growing on DISC can span glial scars (*Figure 5*).

In conclusion, our findings demonstrate decellularization can remove components in normal or injured SC that inhibit axonal regeneration while retaining components that promote repair of SCI. This confirms our view that decellularized tissue (tissue-derived ECM) is a feasible and promising approach to optimize the adverse microenvironment after spinal cord injury, providing a theoretical basis for clinical application of acellular tissue transplantation for repair SCI.

Acknowledgments

Funding: This work was supported by the National Natural Science Foundation of China (No. 32130060 and 82001296), the National Key Research and Development Program of China (No. 2017YFA0104702), the Priority Academic Program Development of Jiangsu Higher Education Institutions (PAPD), and the "226 High-level Talent Training Project" in Nantong City.

Footnote

Reporting Checklist: The authors have completed the ARRIVE reporting checklist. Available at https://atm.amegroups.com/article/view/10.21037/atm-22-3969/rc

Data Sharing Statement: Available at https://atm.amegroups.com/article/view/10.21037/atm-22-3969/dss

Conflicts of Interest: All authors have completed the ICMJE uniform disclosure form (available at https://atm.amegroups.com/article/view/10.21037/atm-22-3969/coif). The authors have no conflicts of interest to declare.

Ethical Statement: The authors are accountable for all aspects of the work in ensuring that questions related to the accuracy or integrity of any part of the work are appropriately investigated and resolved. All animal experimental procedures and protocols were performed under a project license (No. S20210302-037) granted by the Nantong University Animal Experimental Ethics Committee, in compliance with the Institutional Animal Care and Use Committee (IACUC) of Nantong University.

References

1. Sofroniew MV. Dissecting spinal cord regeneration. Nature 2018;557:343-50.
2. Rowland JW, Hawryluk GW, Kwon B, et al. Current status of acute spinal cord injury pathophysiology and emerging therapies: promise on the horizon. Neurosurg Focus 2008;25:E2.
3. Fan B, Wei Z, Yao X, et al. Microenvironment Imbalance of Spinal Cord Injury. Cell Transplant 2018;27:853-66.
4. Schwab ME, Caroni P. Antibody against myelin-associated inhibitor of neurite growth neutralizes nonpermissive substrate properties of CNS white matter. Neuron 2008;60:404-5.
5. Bandtlow CE, Schwab ME. NI-35/250/nogo-a: a neurite growth inhibitor restricting structural plasticity and regeneration of nerve fibers in the adult vertebrate CNS. Glia 2000;29:175-81.
6. Siebert JR, Conta Steencken A, Osterhout DJ. Chondroitin sulfate proteoglycans in the nervous system: inhibitors to repair. Biomed Res Int 2014;2014:845323.
7. Stephenson EL, Zhang P, Ghorbani S, et al. Targeting the Chondroitin Sulfate Proteoglycans: Evaluating Fluorinated Glucosamines and Xylosides in Screens Pertinent to Multiple Sclerosis. ACS Cent Sci 2019;5:1223-34.
8. Jones LL, Sajed D, Tuszynski MH. Axonal regeneration through regions of chondroitin sulfate proteoglycan deposition after spinal cord injury: a balance of permissiveness and inhibition. J Neurosci 2003;23:9276-88.
9. Li G, Che MT, Zhang K, et al. Graft of the NT-3 persistent delivery gelatin sponge scaffold promotes axon regeneration, attenuates inflammation, and induces cell migration in rat and canine with spinal cord injury. Biomaterials 2016;83:233-48.
10. Li X, Fan C, Xiao Z, et al. A collagen microchannel

scaffold carrying paclitaxel-liposomes induces neuronal differentiation of neural stem cells through Wnt/β-catenin signaling for spinal cord injury repair. Biomaterials 2018;183:114-27.
11. Xing H, Ren X, Yin H, et al. Construction of a NT-3 sustained-release system cross-linked with an acellular spinal cord scaffold and its effects on differentiation of cultured bone marrow mesenchymal stem cells. Mater Sci Eng C Mater Biol Appl 2019;104:109902.
12. Yang Y, Fan Y, Zhang H, et al. Small molecules combined with collagen hydrogel direct neurogenesis and migration of neural stem cells after spinal cord injury. Biomaterials 2021;269:120479.
13. Álvarez Z, Kolberg-Edelbrock AN, Sasselli IR, et al. Bioactive scaffolds with enhanced supramolecular motion promote recovery from spinal cord injury. Science 2021;374:848-56.
14. Badylak SF, Freytes DO, Gilbert TW. Extracellular matrix as a biological scaffold material: Structure and function. Acta Biomater 2009;5:1-13.
15. Zhu J, Lu Y, Yu F, et al. Effect of decellularized spinal scaffolds on spinal axon regeneration in rats. J Biomed Mater Res A 2018;106:698-705.
16. Xu ZX, Zhang LQ, Wang CS, et al. Acellular Spinal Cord Scaffold Implantation Promotes Vascular Remodeling with Sustained Delivery of VEGF in a Rat Spinal Cord Hemisection Model. Curr Neurovasc Res 2017;14:274-89.
17. Cerqueira SR, Lee YS, Cornelison RC, et al. Decellularized peripheral nerve supports Schwann cell transplants and axon growth following spinal cord injury. Biomaterials 2018;177:176-85.
18. Bai YR, Lai BQ, Han WT, et al. Decellularized optic nerve functional scaffold transplant facilitates directional axon regeneration and remyelination in the injured white matter of the rat spinal cord. Neural Regen Res 2021;16:2276-83.
19. Hong JY, Seo Y, Davaa G, et al. Decellularized brain matrix enhances macrophage polarization and functional improvements in rat spinal cord injury. Acta Biomater 2020;101:357-71.
20. Buckenmeyer MJ, Meder TJ, Prest TA, et al. Decellularization techniques and their applications for the repair and regeneration of the nervous system. Methods 2020;171:41-61.
21. Crapo PM, Medberry CJ, Reing JE, et al. Biologic scaffolds composed of central nervous system extracellular matrix. Biomaterials 2012;33:3539-47.
22. Sun JH, Li G, Wu TT, et al. Decellularization optimizes the inhibitory microenvironment of the optic nerve to support neurite growth. Biomaterials 2020;258:120289.
23. Leibinger M, Zeitler C, Gobrecht P, et al. Transneuronal delivery of hyper-interleukin-6 enables functional recovery after severe spinal cord injury in mice. Nat Commun 2021;12:391.
24. Wang S, Zhu C, Zhang B, et al. BMSC-derived extracellular matrix better optimizes the microenvironment to support nerve regeneration. Biomaterials 2022;280:121251.
25. Gu Y, Zhu J, Xue C, et al. Chitosan/silk fibroin-based, Schwann cell-derived extracellular matrix-modified scaffolds for bridging rat sciatic nerve gaps. Biomaterials 2014;35:2253-63.
26. Gaudet AD, Popovich PG. Extracellular matrix regulation of inflammation in the healthy and injured spinal cord. Exp Neurol 2014;258:24-34.
27. Theocharis AD, Manou D, Karamanos NK. The extracellular matrix as a multitasking player in disease. FEBS J 2019;286:2830-69.
28. Walker C, Mojares E, Del Río Hernández A. Role of Extracellular Matrix in Development and Cancer Progression. Int J Mol Sci 2018;19:3028.
29. Sonbol HS. Extracellular Matrix Remodeling in Human Disease. J Microsc Ultrastruct 2018;6:123-8.
30. Quraishe S, Forbes LH, Andrews MR. The Extracellular Environment of the CNS: Influence on Plasticity, Sprouting, and Axonal Regeneration after Spinal Cord Injury. Neural Plast 2018;2018:2952386.
31. Hussey GS, Dziki JL, Badylak SF. Extracellular matrix-based materials for regenerative medicine. Nature Reviews Materials 2018;3:159-73.
32. Volpato FZ, Führmann T, Migliaresi C, et al. Using extracellular matrix for regenerative medicine in the spinal cord. Biomaterials 2013;34:4945-55.
33. Dauth S, Grevesse T, Pantazopoulos H, et al. Extracellular matrix protein expression is brain region dependent. J Comp Neurol 2016;524:1309-36.
34. Haggerty AE, Marlow MM, Oudega M. Extracellular matrix components as therapeutics for spinal cord injury. Neurosci Lett 2017;652:50-5.
35. Burnside ER, Bradbury EJ. Manipulating the extracellular matrix and its role in brain and spinal cord plasticity and repair. Neuropathol Appl Neurobiol 2014;40:26-59.
36. Bradbury EJ, Burnside ER. Moving beyond the glial scar for spinal cord repair. Nat Commun 2019;10:3879.
37. Nagai J, Takaya R, Piao W, et al. Deletion of Crmp4 attenuates CSPG-induced inhibition of axonal growth and induces nociceptive recovery after spinal cord injury. Mol

Cell Neurosci 2016;74:42-8.
38. Gensel JC, Zhang B. Macrophage activation and its role in repair and pathology after spinal cord injury. Brain Res 2015;1619:1-11.
39. Zhu Y, Soderblom C, Trojanowsky M, et al. Fibronectin Matrix Assembly after Spinal Cord Injury. J Neurotrauma 2015;32:1158-67.
40. Wiese S, Faissner A. The role of extracellular matrix in spinal cord development. Exp Neurol 2015;274:90-9.
41. Haylock-Jacobs S, Keough MB, Lau L, et al. Chondroitin sulphate proteoglycans: extracellular matrix proteins that regulate immunity of the central nervous system. Autoimmun Rev 2011;10:766-72.
42. Jones LL, Margolis RU, Tuszynski MH. The chondroitin sulfate proteoglycans neurocan, brevican, phosphacan, and versican are differentially regulated following spinal cord injury. Exp Neurol 2003;182:399-411.
43. Bartus K, James ND, Bosch KD, et al. Chondroitin sulphate proteoglycans: key modulators of spinal cord and brain plasticity. Exp Neurol 2012;235:5-17.
44. Schulz M, Diehl V, Trebicka J, et al. Biglycan: A regulator of hepatorenal inflammation and autophagy. Matrix Biol 2021;100-101:150-61.
45. Klimaschewski L, Obermüller N, Witzgall R. Regulation of clusterin expression following spinal cord injury. Cell Tissue Res 2001;306:209-16.
46. Apostolova I, Irintchev A, Schachner M. Tenascin-R restricts posttraumatic remodeling of motoneuron innervation and functional recovery after spinal cord injury in adult mice. J Neurosci 2006;26:7849-59.
47. Esmaeili M, Berry M, Logan A, et al. Decorin treatment of spinal cord injury. Neural Regen Res 2014;9:1653-6.
48. Yokota K, Kobayakawa K, Saito T, et al. Periostin Promotes Scar Formation through the Interaction between Pericytes and Infiltrating Monocytes/Macrophages after Spinal Cord Injury. Am J Pathol 2017;187:639-53.

(English Language Editor: B. Draper)

Cite this article as: Hu J, Shangguan J, Askar P, Xu J, Sun H, Zhou S, Zhu C, Su W, Gu Y. Decellularization alters the unfavorable regenerative adverse microenvironment of the injured spinal cord to support neurite outgrowth. Ann Transl Med 2022;10(17):934. doi: 10.21037/atm-22-3969

